

**Downward Terrestrial Gamma-Ray Flash Observed in a Winter Thunderstorm**Y. Wada,<sup>1,2</sup> T. Enoto,<sup>3,2</sup> K. Nakazawa,<sup>4</sup> Y. Furuta,<sup>5</sup> T. Yuasa,<sup>6</sup> Y. Nakamura,<sup>7</sup> T. Morimoto,<sup>8</sup>  
T. Matsumoto,<sup>1</sup> K. Makishima,<sup>1,2,9</sup> and H. Tsuchiya<sup>10</sup><sup>1</sup>*Department of Physics, Graduate School of Science, The University of Tokyo, 7-3-1 Hongo, Bunkyo-ku, Tokyo 113-0033, Japan*<sup>2</sup>*High Energy Astrophysics Laboratory, Nishina Center for Accelerator-Based Science, RIKEN, 2-1 Hirosawa, Wako, Saitama 351-0198, Japan*<sup>3</sup>*The Hakubi Center for Advanced Research and Department of Astronomy, Kyoto University, Kitashirakawa Oiwake-cho, Sakyo-ku, Kyoto, Kyoto 606-8502, Japan*<sup>4</sup>*Kobayashi-Maskawa Institute for the Origin of Particles and the Universe, Nagoya University, Furo-cho, Chikusa-ku, Nagoya, Aichi 464-8601, Japan*<sup>5</sup>*Collaborative Laboratories for Advanced Decommissioning Science, Japan Atomic Energy Agency, 2-4 Shirakata, Tokai-mura, Naka-gun, Ibaraki 319-1195, Japan*<sup>6</sup>*Block 4B, Boon Tiong Road, Singapore 165004, Singapore*<sup>7</sup>*Kobe City College of Technology, 8-3 Gakuen-Higashimachi, Nishi-ku, Kobe, Hyogo 651-2194, Japan*<sup>8</sup>*Faculty of Science and Engineering, Kindai University, 3-4-1 Kowakae, Higashiosaka, Osaka 577-8502, Japan*<sup>9</sup>*Kavli Institute for the Physics and Mathematics of the Universe, The University of Tokyo, 5-1-5 Kashiwa-no-ha, Kashiwa, Chiba 277-8683, Japan*<sup>10</sup>*Nuclear Science and Engineering Center, Japan Atomic Energy Agency, 2-4 Shirakata, Tokai-mura, Naka-gun, Ibaraki 319-1195, Japan*

(Received 5 March 2019; revised manuscript received 19 May 2019; published 7 August 2019)

During a winter thunderstorm on 24 November 2017, a strong burst of gamma rays with energies up to  $\sim 10$  MeV was detected coincident with a lightning discharge, by scintillation detectors installed at the Kashiwazaki-Kariwa Nuclear Power Station at sea level in Japan. The burst had a subsecond duration, which is suggestive of photoneutron production. The leading part of the burst was resolved into four intense gamma-ray bunches, each coincident with a low-frequency radio pulse. These bunches were separated by 0.7–1.5 ms, with a duration of  $\ll 1$  ms each. Thus, the present burst may be considered as a “downward” terrestrial gamma-ray flash (TGF), which is analogous to upgoing TGFs observed from space. Although the scintillation detectors were heavily saturated by these bunches, the total dose associated with them was successfully measured by ionization chambers, employed by nine monitoring posts surrounding the power plant. From this information and Monte Carlo simulations, the present downward TGF is suggested to have taken place at an altitude of  $2500 \pm 500$  m, involving  $8_{-4}^{+8} \times 10^{18}$  avalanche electrons with energies above 1 MeV. This number is comparable to those in upgoing TGFs.

DOI: [10.1103/PhysRevLett.123.061103](https://doi.org/10.1103/PhysRevLett.123.061103)

**Introduction.**—Terrestrial gamma-ray flashes (TGFs) are submillisecond gamma-ray emissions coincident with lightning discharges. Since their discovery in 1991 [1], TGFs have been observed by gamma-ray astronomy satellites [2–7] and by aircraft [8,9]. The TGF photons, reaching 20 MeV or higher [2,4], originate from bremsstrahlung by energetic electrons. These electrons are thought to be accelerated by the relativistic runaway electron avalanche (RREA) mechanism [10,11] in strong electric fields of lightning and multiplied via such processes as the relativistic feedback processes [12] or the leader-seeded processes [13,14].

Ground-level observations of natural [15–18] and rocket-triggered [19,20] lightning have discovered gamma-ray flashes, similar to TGFs but beamed downward. These bursts, called downward TGFs, indeed have characteristics

common with ordinary TGFs, such as coincidence with lightning, submillisecond duration, and photon energies of  $> 10$  MeV. Recently, several downward TGFs in winter thunderstorms have been found to be so intense as to cause atmospheric photonuclear reactions, such as  $^{14}\text{N} + \gamma \rightarrow ^{13}\text{N} + n$  [21–23].

Since downward TGFs take place close to the ground, brighter ones with high gamma-ray fluxes can heavily saturate detectors [20]. In particular, those bright enough to produce observable numbers of photoneutrons completely exceeded the counting capabilities of typical scintillation detectors [21–23]. As a result, we have not been able to estimate the gamma-ray fluence of downward TGFs that involve photonuclear reactions. Here we report on the detection, with scintillation detectors, of a downward TGF which triggered photonuclear reactions and estimate the

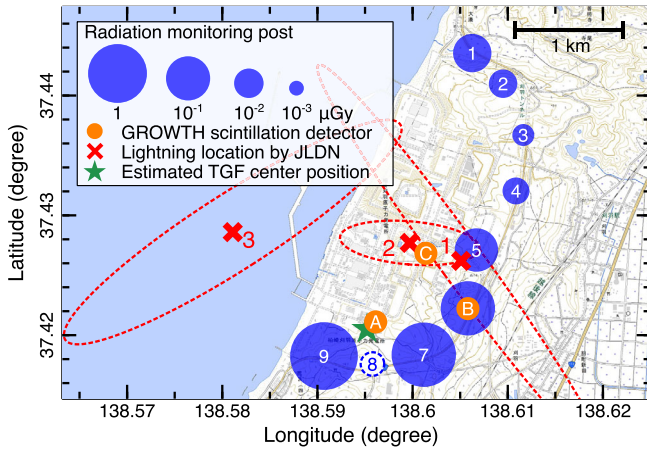


FIG. 1. Locations of the detectors in the Kashiwazaki-Kariwa Nuclear Power Station. Orange circles show detectors A–C, blue circles monitoring posts (MPs), and the green star the estimated position where the TGF took place. The size of the blue circles indicates the dose of the present TGF. Red crosses and dashed-line ellipses show the positions of lightning discharges and their errors reported by JLDN, respectively. The numbers 1–3 indicate the time order of these discharges, as shown in Fig. 2(h). Detector B and MP6 are installed cospatial. The MP8 data were unavailable in the present study.

gamma-ray fluence using ionization chambers tolerant to high-flux radiation.

**Instruments.**—We have been performing the gamma-ray observation of winter thunderclouds (GROWTH) experiment in coastal areas of the Japan Sea [23–28]. The present observation was performed in the Kashiwazaki-Kariwa Nuclear Power Station, one of GROWTH’s sites. This site, successfully operated since December 2006, was enhanced in 2016, with three gamma-ray detectors (detectors A–C), of which the locations are shown in Fig. 1.

Detectors A, B, and C employ a  $\text{Bi}_4\text{Ge}_3\text{O}_{12}$  (BGO) crystal scintillator of  $25.0 \times 8.0 \times 2.5 \text{ cm}^3$  each and are sensitive to 0.2–18.0, 0.2–26.0, and 0.3–15.0 MeV gamma rays, respectively. Scintillation pulses from these BGO crystals are read by phototubes. Analog outputs from each phototube are processed by a charge amplifier and a shaping amplifier, with time constants of 10 and 2  $\mu\text{s}$ , respectively. The amplified analog waveforms are sampled by our original data acquisition (DAQ) system with 50 MHz analog-to-digital converters [23,28]. Once the DAQ system detects a pulse, it stores the digitized pulse waveform during a 20  $\mu\text{s}$  gate time and measures its maximum and minimum values. The maximum value, corresponding to the pulse height, is converted into the deposited energy in the crystal via energy calibration. Minimum values present the baseline of the analog outputs and normally remain  $\sim 0 \text{ V}$ . The DAQ system can count pulses up to 10 kHz properly. The absolute timing of the detectors is adjusted by global-positioning-system signals to an accuracy of  $< 1 \mu\text{s}$ .

In addition, radiation monitoring posts (MPs), operated by the power station and distributed as in Fig. 1, measure dose rates every 30 s. Each station consists of a  $\phi 5.1 \text{ cm} \times 5.1 \text{ cm}$  NaI scintillation detector (NaI) and an ionization chamber (IC), a sphere of 2-mm-thick stainless steel filled with 14-L argon gas at 4 atm. These NaIs and ICs are sensitive to gamma rays of 0.05–3.0 MeV and  $> 0.05 \text{ MeV}$ , respectively. While NaIs are dedicated to low-dose-rate measurements up to  $10 \mu\text{Gy h}^{-1}$ , ICs stand high rates up to  $100 \mu\text{Gy h}^{-1}$ .

Lightning activities are monitored by a broadband low-frequency (LF) radio receiver which we installed at Nyuzen ( $36.954^\circ\text{N}$ ,  $137.498^\circ\text{E}$ ), 110 km west-southwest from the observation site. The LF receiver consists of a flat-plate antenna sensitive to the 0.8–500 kHz band. Analog outputs from the antenna are sampled by a 4 MHz digitizer [29]. We also utilize commercial information of the Japan Lightning Detection Network (JLDN), to obtain the position, timing, discharge current, and classification (cloud to ground or in cloud) of lightning pulses.

**Results.**—During a thunderstorm on 24 November 2017, we observed a lightning discharge and a radiation burst simultaneously, at 10:03:02.282827 UTC, which we hereafter employ as the origin of the elapsed time. Figures 2(a)–2(c) present the time series of count rates obtained by detectors A–C, respectively, and Fig. 2(d) an LF waveform which continued for  $\sim 400 \text{ ms}$ . The gamma-ray burst had a steep onset ( $< 10 \text{ ms}$ ) coincident with the lightning discharge, followed by an exponential decay with a time constant of 59, 47, and 48 ms for detectors A, B, and C, respectively. As shown in Enoto *et al.* [23], these decay constants are consistent with those of neutron thermalization and subsequent emission of deexcitation gamma rays through neutron captures (mainly  $^{14}\text{N} + n \rightarrow ^{15}\text{N} + \gamma$ ). In addition, detector A detected an afterglow, lasting for  $\sim 10 \text{ s}$  and mainly consisting of 511-keV annihilation photons. This is due to positrons emitted from  $\beta^+$ -decaying nuclei such as  $^{13}\text{N}$  [23]. Therefore, we infer that photonuclear reactions such as  $^{14}\text{N} + \gamma \rightarrow ^{13}\text{N} + n$  occurred following the lightning discharge.

Figures 2(e)–2(g) expand the initial phase of the gamma-ray burst, where the maximum and minimum values of the analog outputs measured every 20  $\mu\text{s}$  are plotted in a photon-by-photon basis. During  $0 < t < 5 \text{ ms}$ , the maximum values of several photons exceeded the saturation level of the analog amplifier ( $\sim 4 \text{ V}$ ). At the same time, the minimum values went significantly negative and gradually returned to their normal baseline level. This behavior, called “baseline undershoot,” is most clearly seen in Figs. 2(e) and 2(g). These saturated pulses and baseline undershoots are caused when large charge pulses from the phototube are fed into the charge amplifier. As in Ref. [23], this provides clear evidence of a downward TGF, namely, large energy deposits into the BGO crystals in  $< 1 \text{ ms}$ .

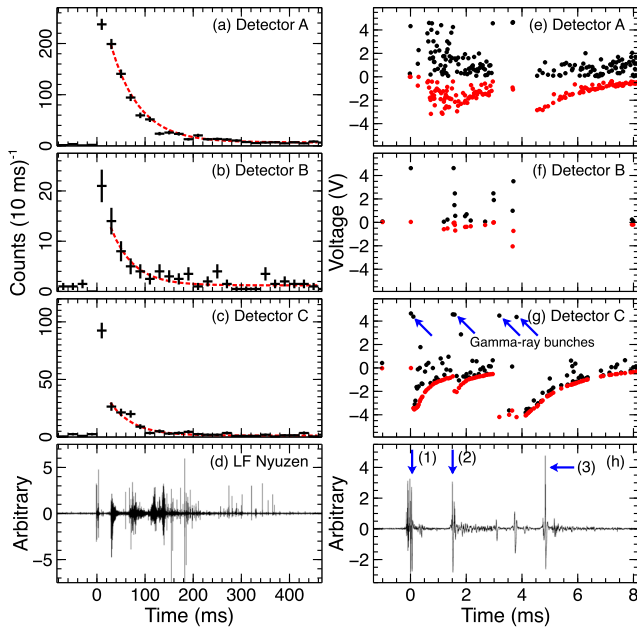


FIG. 2. (a)–(c) Count-rate histories of detectors A–C with 10-ms bins. Overlaid red lines show the best-fit exponential functions. (d) An LF waveform obtained by the Nyuzen station, corrected for the propagation time from the station to the detector site. (e)–(g) An expanded time series over  $-1 < t < 8$  ms. Each gamma-ray photon is represented by a pair of black and red dots, which means the maximum and minimum analog voltage from the shaping amplifier output (see the text). Blue arrows in (g) show the four gamma-ray bunches. (h) An expansion of (d). The timings of pulses reported by JLDN are presented by blue arrows. The number of pulses corresponds to that in Fig. 1.

In Fig. 2(g), the saturated signals of detector C, accompanied by the undershoots, can be recognized on four occasions, at  $t \sim 0.0$ , 1.5, 3.1, and 3.7 ms. The same effects, though less obvious, are seen by detectors A and B. Therefore, the downward TGF is considered to consist of four gamma-ray “bunches” with a duration of  $< 1$  ms each, and each of them reached our three detectors simultaneously. The interval between adjacent bunches ranges over 0.71–1.52 ms, on average 1.22 ms.

Although these bunches must contain a large number of gamma-ray photons, our DAQ system can record only one photon event during each 20  $\mu$ s gate time, even if multiple photons arrive in this period. Furthermore, once saturated, our charge amplifiers take  $\sim 1$  ms to recover from the negative undershoot [Fig. 2(g)]. The forefront of this interval becomes a dead time, in which subsequent events cannot be acquired. Thus, our detectors were not able to resolve these bunches into individual photons. Instead, we can use the saturated signals as the onset of a gamma-ray bunch. As the negative undershoot becomes  $\geq -3$  V, the detectors resume detecting the photons (mainly from the neutron capture processes), but their pulse heights can be incorrect by at least  $t \sim 10$  ms.

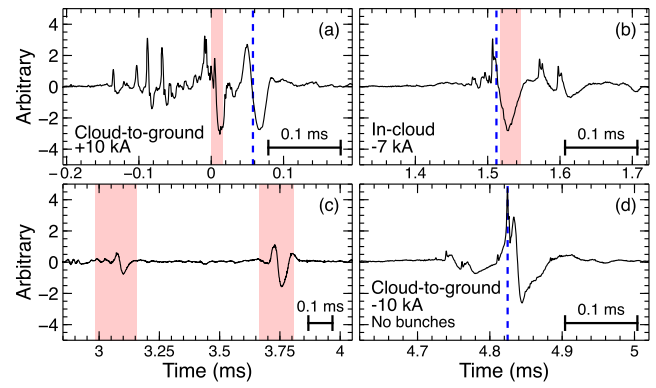


FIG. 3. Expanded LF waveforms of Fig. 2(h). Timing of the lightning discharges reported by JLDN are indicated with blue dashed lines. The estimated onset timing of each gamma-ray bunch is shown by the red-shaded region, of which the width reflects differences among the three scintillators. As is customary with atmospheric electricity, pulses with a positive onset indicate negative polarity, namely, downward negative current or upward positive current.

Figure 2(h) expands the LF waveform. Over  $0 < t < 6$  ms, when the bunches were detected, we notice 5–6 LF spikes. The highest three of them are coincident with discharges reported by JLDN, a cloud-to-ground pulse of +10 kA at  $t \sim 0.06$  ms, an in-cloud pulse ( $-7$  kA,  $t \sim 1.51$  ms), and a cloud-to-ground pulse ( $-10$  kA,  $t \sim 4.82$  ms), indicated as (1), (2), and (3) in Fig. 2(h), respectively. Their positions reported by JLDN are shown in Fig. 1. The first two of them coincide with the first two gamma-ray bunches, and, furthermore, two smaller LF pulses at  $t \sim 3.1$  and 3.7 ms, though too faint for JLDN, are approximately coincident with the third and fourth bunches. In contrast, we observed no gamma-ray bunches coincident with the third JLDN-reported pulse.

To examine the suggested association between the LF pulses and the gamma-ray bunches, we further expand, in Fig. 3, the five pulses in Fig. 2(h), where the onset timing of the four gamma-ray bunches are also displayed. The first bunch at  $t = 0.0$  ms took place with a positive LF pulse, which followed a train of negative-polarity fast pulses in  $-0.14 < t < 0.0$  ms, namely, stepped leaders, and preceded the return stroke at  $t = 0.58$  ms which JLDN reported. The second bunch coincides with a JLDN-reported in-cloud pulse. The third and fourth bunches are also correlated with LF pulses which have bipolar shapes. However, the onset timings of these bunches have larger uncertainties by 0.1–0.2 ms, which are caused probably because the trigger timing of the subsequent bunch is affected by the charge amplifier recovery from the preceding bunch.

Besides detectors A–C, eight ICs also detected the entire burst, in the form of a clear increase in their 30-s dose rates. In particular, those at MP9 and MP6 reached 170 and 25  $\mu$ Gy  $\text{h}^{-1}$ , respectively. After subtracting the environmental background, the IC doses integrated for 30 s become 1.4

and  $0.2 \mu\text{Gy}$ , respectively (Fig. 1). Assuming a bunch duration as  $<1 \text{ ms}$  ( $<4 \text{ ms}$  in total), the instantaneous dose rates reach  $1.3$  and  $0.2 \text{ Gy h}^{-1}$ , respectively. The data of MP8 were unavailable, because it temporarily went down just after the lightning discharge. Since ICs have a tolerance for high gamma-ray fluxes by measuring accumulated doses instead of counting photons, their increases must be contributed by both the downward TGF (the four bunches) and the subsecond emission component.

A slight dose increase, by  $\sim 10^{-4} \mu\text{Gy}$  or less, was also detected by NaIs. Being typical scintillation detectors, they also failed to properly count gamma rays in the bunches and, hence, have measured doses only of the subsecond component, which originates from neutron captures [23] and contains multiple emission lines up to  $10.8 \text{ MeV}$ . By extrapolating from the  $0.05\text{--}3.0 \text{ MeV}$  NaI doses, those up to  $10.8 \text{ MeV}$  were estimated as  $2 \times 10^{-3} \mu\text{Gy}$  at MP9, which is  $<1\%$  of the actually measured IC doses. Therefore, we conclude that the IC dose increases were caused predominantly by the downward TGF rather than by the subsecond emission from neutrons. In the same way, doses by the direct neutrons are negligible. The present gamma-ray burst, as a whole, is inferred to have involved a  $>100$  times larger number of gamma-ray photons than those apparently recorded in Figs. 2(e)–2(g).

*Monte Carlo simulations.*—To quantify the present downward TGF, we performed Monte Carlo simulations with GEANT4 [30]. As a preliminary attempt, we irradiated a mass model of IC with  $0.05\text{--}50 \text{ MeV}$  gamma rays, which follow a spectrum as  $E^{-1} \exp(-E/7.3 \text{ MeV})$ , with  $E$  being the gamma-ray energy, as expected for bremsstrahlung emission by avalanche electrons [31]. Then, a typical IC dose,  $0.050 \mu\text{Gy}$ , was found to correspond to a gamma-ray fluence of  $10^4 \text{ photons cm}^{-2}$ . This calibration gives the fluences at MP9 and MP6 as  $2.8 \times 10^5$  and  $4.2 \times 10^4 \text{ photons cm}^{-2}$ , respectively. The present TGF spectrum, although not measured by our detectors, could have had an additional power-law component at higher energies [4,32]. Its inclusion into this simulation, with parameters fixed to those of Tavani *et al.* [4], was found to increase the fluences necessary to explain the IC doses by only  $\sim 30\%$  or less. Further assuming the total TGF duration conservatively as  $<10 \text{ ms}$ , the gamma-ray fluxes which arrived at MP9 and MP6 are estimated as  $>2.8 \times 10^7$  and  $>0.4 \times 10^7 \text{ photons cm}^{-2} \text{ s}^{-1}$ , respectively. Although similar fluxes must have arrived at detectors A–C, the peak gamma-ray fluxes they actually measured are at most  $\sim 300 \text{ photons cm}^{-2} \text{ s}^{-1}$  (from their effective areas and Fig. 1). Thus, we conclude that the present TGF had a gamma-ray flux which is  $10^4\text{--}10^5$  times higher than those apparently recorded by detectors A–C and completely saturated them.

Then, we performed full simulations starting from electrons. A two-stage simulation was employed for computational economy. In the first stage, initial particles,

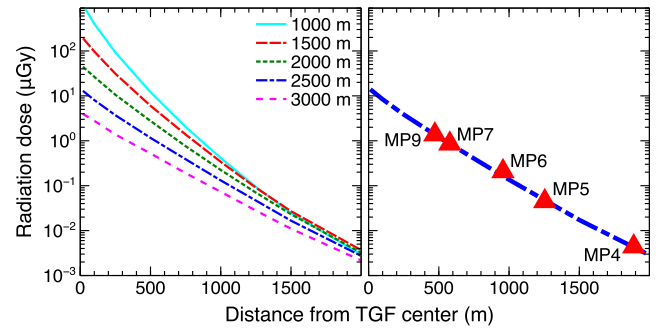


FIG. 4. Results of Monte Carlo simulations. (Left) Air absorbed doses shown as a function of the offset from the TGF center. Different colors specify different initial heights of injected electrons. The obtained doses are normalized to an electron number of  $8 \times 10^{18}$  above  $1 \text{ MeV}$ . (Right) The best-fitting model to the IC data (see the text).

namely, avalanche electrons, were injected in a mass model of the atmosphere, to simulate their atmospheric interactions and track their bremsstrahlung gamma rays. Information of the gamma rays, such as the energy, position, and momentum vector, was collected when they reached the ground. In the second stage, the gamma rays reaching the ground were input into the IC mass model, like in the preliminary examination.

In the above simulation, the initial electrons were assumed to follow the theoretical spectrum of RREA,  $\exp(-\epsilon/7.3 \text{ MeV})$  [33], where  $\epsilon$  is the electron energy. The electron beam is assumed to be narrow and downward, with neither a tilt angle nor beam divergence. At an altitude from  $1000$  to  $3000 \text{ m}$  with a  $250\text{-m}$  step,  $10^9$  electrons of  $1\text{--}50 \text{ MeV}$  were injected. Initial electrons below  $1 \text{ MeV}$  were ignored, because their products are mostly absorbed before reaching the ground. The left panel in Fig. 4 shows the results from these simulations, in the form of a lateral spread of gamma-ray doses, as caused by struggling of electrons and scatterings of bremsstrahlung photons.

The Monte Carlo predicted doses at each altitude were compared with the IC measurements at different locations. By changing the TGF center position with the  $50\text{-m}$  step and using the IC data (including  $15\%$  systematic errors) within  $2000 \text{ m}$  of the assumed TGF center, we searched for the best-fit solution via chi-square evaluation. Then, as shown in the right panel in Fig. 4, the fitting has become acceptable with  $\chi^2 = 2.19$  for 1 degree of freedom (five data points and four parameters, namely, the two-dimensional position, altitude, and normalization), for the total avalanche electrons above  $1 \text{ MeV}$  of  $8_{-4}^{+8} \times 10^{18}$ , the TGF height of  $2500 \pm 500 \text{ m}$  altitude, and the TGF center being  $100 \text{ m}$  southwest from detector A (Fig. 1). Errors are at a  $1\sigma$  confidence level. The on-ground fluences of  $>1 \text{ MeV}$  gamma rays from the four bunches are estimated as  $4 \times 10^5 \text{ photons cm}^{-2}$  at the TGF center and  $7 \times 10^3 \text{ photons cm}^{-2}$  at an offset of  $1 \text{ km}$ .

*Discussion.*—The present burst can be understood as a downward TGF, which consisted of the four gamma-ray bunches like multipulse TGFs observed from space [34]. The intervals between adjacent bunches in the present case, a few milliseconds, are similar to those of multipulse TGFs [1,34]. As seen in Fig. 3(a), the first bunch took place at the last phase of the leader development, in agreement with several previous reports [18,22,35,36]. Since the LF pulses for  $-0.15 < t < 0$  ms are negative, the relevant leaders must be downward negative ones or upward positive ones. In either case, electrons should be accelerated downward, as required for the occurrence of downward TGFs. In addition, the first bunch clearly preceded the return stroke. This agrees with a simple physical expectation that electrostatic acceleration should be hampered in return strokes, due to the azimuthal magnetic field created by the strong electric current. The other bunches, though coincident with negative LF pulses, also have less clear relations to return strokes of cloud-to-ground currents.

Ordinary TGFs, observed from space, typically initiate at altitudes of  $\geq 8$  km [7,36], namely, in the middle to upper layers of summertime thunderclouds. In contrast, the estimated altitude of  $2.5 \pm 0.5$  km in the present case is much lower, where the atmosphere is approximately twice denser. Since winter thunderstorms in Japan typically have  $\sim 5$  km cloud tops and  $< 1$  km cloud bases [37], the present TGF is likely to have taken place in a lower to middle layer of the winter thunderclouds.

Using TGF data obtained by Reuven Ramaty High Energy Solar Spectroscopic Imager, Dwyer and Smith [38] estimated the number of involved electrons ( $> 1$  MeV) as  $1 \times 10^{16} - 2 \times 10^{17}$ , and Mailyan *et al.* [7], using individual Fermi TGF data, derived as  $4 \times 10^{16} - 3 \times 10^{19}$ , with an average of  $2 \times 10^{18}$ . The estimated electron number of the present burst is in the range of Mailyan *et al.* Therefore, the downward TGFs in the present case have approximately the same properties as ordinary TGFs, despite the atmospheric density difference.

During winter thunderstorms in Japan, Bowers *et al.* [21] detected a downward TGF and indirectly estimated its total number of photons above 1 MeV as  $\sim 10^{17}$ , considering that it produced neutrons via photonuclear reactions. The electron number above 1 MeV of our estimation,  $8_{-4}^{+8} \times 10^{18}$ , can be converted into the initial number of bremsstrahlung photons as  $7_{-3}^{+7} \times 10^{17}$ . Therefore, the case of Bowers *et al.* is similar to ours. Furthermore, we succeeded for the first time in directly measuring the doses included in a downward TGF that triggered photonuclear reactions and in evaluating the number of avalanche electrons. At the Kashiwazaki-Kariwa site, we previously observed another gamma-ray burst that involved photonuclear reactions [23]. We infer that this burst is similar to the present one and that of Bowers *et al.* [21], because the

number of photoneutrons in this case is estimated to be of the same order as that of Bowers *et al.*

In summary, we observed, during a winter thunderstorm, a downward TGF consisting of four gamma-ray bunches coincident with LF pulses. The IC doses and the Monte Carlo simulations allowed us to estimate the total number of avalanche electrons as  $8 \times 10^{18}$  above 1 MeV, produced at the 2500 m altitude. The present result suggests that downward TGFs in winter thunderclouds have characteristics very similar to those of upgoing TGFs, except the electrons being accelerated in opposite directions into a much thicker atmosphere.

We thank the radiation safety group of the Kashiwazaki-Kariwa Nuclear Power Station of Tokyo Electric Power Company Holdings for providing the observation site and the MP data. The BGO scintillation crystals were provided by Sakurai Radioactive Isotope Physics Laboratory of RIKEN Nishina Center and Nuclear Experiment Group of The University of Tokyo. We appreciate discussions with T. Torii, M. Ikuta, A. Bamba, H. Odaka, and T. Tamagawa and advice for simulations by G. S. Bowers. The Monte Carlo simulations were performed on the HOKUSAI BigWaterfall supercomputing system of RIKEN Advanced Center for Computing and Communication. The deployment of the LF receiver was supported by the town of Nyuzen, Toyama Prefecture. This research is supported by JSPS/MEXT KAKENHI Grants No. 15K05115, No. 15H03653, No. 16H06006, No. 16K05555, No. 18J13355, No. 18H01236, No. 19H00683, and No. 17K05659, by SPIRITS and Hakubi projects of Kyoto University, by the Hayakawa Satio Fund of the Astronomical Society of Japan, and by citizen supporters via an academic crowdfunding platform “academist.” The background image in Fig. 1 was provided by the Geospatial Information Authority of Japan.

- 
- [1] G. J. Fishman, P. N. Bhat, R. Mallozzi, J. M. Horack, T. Koshut, C. Kouveliotou, G. N. Pendleton, C. A. Meegan, R. B. Wilson, W. S. Paciesas *et al.*, *Science* **264**, 1313 (1994).
  - [2] D. M. Smith, L. I. Lopez, R. P. Lin, and C. P. Barrington-Leigh, *Science* **307**, 1085 (2005).
  - [3] M. Marisaldi, F. Fuschino, C. Labanti, M. Galli, F. Longo, E. Del Monte, G. Barbiellini, M. Tavani, A. Giuliani, E. Moretti *et al.*, *J. Geophys. Res. Space Phys.* **115** (2010).
  - [4] M. Tavani, M. Marisaldi, C. Labanti, F. Fuschino, A. Argan, A. Trois, P. Giommi, S. Colafrancesco, C. Pittori, F. Palma *et al.*, *Phys. Rev. Lett.* **106**, 018501 (2011).
  - [5] M. S. Briggs, G. J. Fishman, V. Connaughton, P. N. Bhat, W. S. Paciesas, R. D. Preece, C. Wilson-Hodge, V. L. Chaplin, R. M. Kippen, A. von Kienlin *et al.*, *J. Geophys. Res. Space Phys.* **115** (2010).
  - [6] M. S. Briggs, V. Connaughton, C. Wilson-Hodge, R. D. Preece, G. J. Fishman, R. M. Kippen, P. N. Bhat, W. S. Paciesas, V. L. Chaplin, C. A. Meegan *et al.*, *Geophys. Res. Lett.* **38** (2011).

- [7] B. G. Mailyan, M. S. Briggs, E. S. Cramer, G. Fitzpatrick, O. J. Roberts, M. Stanbro, V. Connaughton, S. McBreen, P. N. Bhat, and J. R. Dwyer, *J. Geophys. Res. Space Phys.* **121**, 11346 (2016).
- [8] D. M. Smith, J. R. Dwyer, B. J. Hazelton, B. W. Grefenstette, G. F. M. Martinez-McKinney, Z. Y. Zhang, A. W. Lowell, N. A. Kelley, M. E. Splitt, S. M. Lazarus *et al.*, *J. Geophys. Res.* **116** (2011).
- [9] G. S. Bowers, D. M. Smith, N. A. Kelley, G. F. Martinez-McKinney, S. A. Cummer, J. R. Dwyer, S. Heckman, R. H. Holzworth, F. Marks, P. Reasor *et al.*, *J. Geophys. Res.* **123**, 4977 (2018).
- [10] A. Gurevich, G. Milikh, and R. Roussel-Dupre, *Phys. Lett. A* **165A**, 463 (1992).
- [11] J. R. Dwyer, *Geophys. Res. Lett.* **31** (2004).
- [12] J. R. Dwyer, *J. Geophys. Res. Space Phys.* **117** (2012).
- [13] S. Celestin and V. P. Pasko, *J. Geophys. Res. Space Phys.* **116** (2011).
- [14] L. P. Babich, E. I. Bochkov, I. M. Kutsyk, T. Neubert, and O. Chanrion, *J. Geophys. Res. Space Phys.* **120**, 5087 (2015).
- [15] M. Tran, V. Rakov, S. Mallick, J. Dwyer, A. Nag, and S. Heckman, *J. Atmos. Sol. Terr. Phys.* **136**, 86 (2015).
- [16] R. Colalillo, *Proc. Sci.*, ICRC2017 (2017).
- [17] R. Abbasi, M. Abe, T. Abu-Zayyad, M. Allen, R. Anderson, R. Azuma, E. Barcikowski, J. Belz, D. Bergman, S. Blake *et al.*, *Phys. Lett. A* **381**, 2565 (2017).
- [18] R. U. Abbasi, T. Abu-Zayyad, M. Allen, E. Barcikowski, J. W. Belz, D. R. Bergman, S. A. Blake, M. Byrne, R. Cady, B. Cheon *et al.*, *J. Geophys. Res.* **123**, 6864 (2018).
- [19] J. R. Dwyer, H. K. Rassoul, M. Al-Dayeh, L. Caraway, B. Wright, A. Chrest, M. A. Uman, V. A. Rakov, K. J. Rambo, D. M. Jordan *et al.*, *Geophys. Res. Lett.* **31** (2004).
- [20] B. M. Hare, M. A. Uman, J. R. Dwyer, D. M. Jordan, M. I. Biggerstaff, J. A. Caicedo, F. L. Carvalho, R. A. Wilkes, D. A. Kotovsky, W. R. Gamerota *et al.*, *J. Geophys. Res.* **121**, 6511 (2016).
- [21] G. S. Bowers, D. M. Smith, G. F. Martinez-McKinney, M. Kamogawa, S. A. Cummer, J. R. Dwyer, D. Wang, M. Stock, and Z. Kawasaki, *Geophys. Res. Lett.* **44**, 10063 (2017).
- [22] D. M. Smith, G. S. Bowers, M. Kamogawa, D. Wang, T. Ushio, J. Ortberg, J. R. Dwyer, and M. Stock, *J. Geophys. Res.* **123**, 11321 (2018).
- [23] T. Enoto, Y. Wada, Y. Furuta, K. Nakazawa, T. Yuasa, K. Okuda, K. Makishima, M. Sato, Y. Sato, T. Nakano *et al.*, *Nature (London)* **551**, 481 (2017).
- [24] H. Tsuchiya, T. Enoto, S. Yamada, T. Yuasa, M. Kawaharada, T. Kitaguchi, M. Kokubun, H. Kato, M. Okano, S. Nakamura *et al.*, *Phys. Rev. Lett.* **99**, 165002 (2007).
- [25] H. Tsuchiya, T. Enoto, S. Yamada, T. Yuasa, K. Nakazawa, T. Kitaguchi, M. Kawaharada, M. Kokubun, H. Kato, M. Okano *et al.*, *J. Geophys. Res.* **116** (2011).
- [26] H. Tsuchiya, T. Enoto, K. Iwata, S. Yamada, T. Yuasa, T. Kitaguchi, M. Kawaharada, K. Nakazawa, M. Kokubun, H. Kato *et al.*, *Phys. Rev. Lett.* **111**, 015001 (2013).
- [27] D. Umemoto, H. Tsuchiya, T. Enoto, S. Yamada, T. Yuasa, M. Kawaharada, T. Kitaguchi, K. Nakazawa, M. Kokubun, H. Kato *et al.*, *Phys. Rev. E* **93**, 021201(R) (2016).
- [28] Y. Wada, G. S. Bowers, T. Enoto, M. Kamogawa, Y. Nakamura, T. Morimoto, D. M. Smith, Y. Furuta, K. Nakazawa, T. Yuasa *et al.*, *Geophys. Res. Lett.* **45**, 5700 (2018).
- [29] Y. Takayanagi, M. Akita, Y. Nakamura, S. Yoshida, T. Morimoto, T. Ushio, Z.-i. Kawasaki, D. Wang, N. Takagi, H. Sakurano *et al.*, *IEEJ Trans. Fundam. Mater.* **133**, 132 (2013).
- [30] S. Agostinelli, J. Allison, K. Amako, J. Apostolakis, H. Araujo, P. Arce, M. Asai, D. Axen, S. Banerjee, G. Barrand *et al.*, *Nucl. Instrum. Methods Phys. Res., Sect. A* **506**, 250 (2003).
- [31] J. R. Dwyer, D. M. Smith, and S. A. Cummer, *Space Sci. Rev.* **173**, 133 (2012).
- [32] S. Celestin, W. Xu, and V. P. Pasko, *J. Geophys. Res. Space Phys.* **117** (2012).
- [33] J. R. Dwyer and L. P. Babich, *J. Geophys. Res. Space Phys.* **116** (2011).
- [34] S. Foley, G. Fitzpatrick, M. S. Briggs, V. Connaughton, D. Tierney, S. McBreen, J. R. Dwyer, V. L. Chaplin, P. N. Bhat, D. Byrne *et al.*, *J. Geophys. Res. Space Phys.* **119**, 5931 (2014).
- [35] G. Lu, R. J. Blakeslee, J. Li, D. M. Smith, X.-M. Shao, E. W. McCaul, D. E. Buechler, H. J. Christian, J. M. Hall, and S. A. Cummer, *Geophys. Res. Lett.* **37** (2010).
- [36] S. A. Cummer, F. Lyu, M. S. Briggs, G. Fitzpatrick, O. J. Roberts, and J. R. Dwyer, *Geophys. Res. Lett.* **42**, 7792 (2015).
- [37] N. Kitagawa, *Research letters on atmospheric electricity* **12**, 143 (1992).
- [38] J. R. Dwyer and D. M. Smith, *Geophys. Res. Lett.* **32** (2005).